JOURNAL OF Applied Polymer SCIENCE

Preparation and Characterization of Thin Film Composite Membranes Modified with Amine-Functionalized β-Cyclodextrins

Bhekani S. Mbuli,[1] Derrick S. Dlamini,[1] Edward N. Nxumalo,[1] Rui W. Krause,[1] Visvanathan L. Pillay,[2] Yoram Oren,[3] Charles Linder,[3] Bhekie B. Mamba[1]

[1]Department of Applied Chemistry, University of Johannesburg, P.O. Box 17011, Doornfontein 2028, South Africa
[2]Department of Chemical Engineering, Durban University of Technology, P.O. Box 1334, Durban, South Africa
[3]Department of Desalination and Water Treatment, Zuckerberg Institute for Water Research, Ben-Gurion University of the Negev, P.O. Box 653, Beer-Sheva 84109, Israel
Correspondence to: B. B. Mamba (E-mail: bmamba@uj.ac.za)

ABSTRACT: This article describes the preparation and characterization of thin film composite (TFC) membranes for the treatment of water by desalination and removal of organic pollutants. The TFC membranes were prepared using trimesoyl chloride and *m*-phenyldiamine. Amine-functionalized β-cyclodextrins (CDs) were added to modify membrane flux and rejection. Contact angle measurements demonstrate that the incorporation of the functionalized CDs increased the hydrophilicity of the membrane. All the modified membranes showed improved fluxes with a maximum of 20 L m^{-2} h^{-1} compared to 5.59 L m^{-2} h^{-1} for the unmodified membranes at a pressure of 100 psi. Further, improved fluxes and salt rejections were achieved (maximum NaCl and Na_2SO_4 salt rejections were 86% and 94.7%, respectively). Thus, the incorporation of functionalized CDs into TFC membranes improves both the hydrophilicity for minimizing fouling and the rejection of salts without loss of flux. © 2012 Wiley Periodicals, Inc. J. Appl. Polym. Sci. 000: 000–000, 2012

KEYWORDS: composites; hydrophilic polymers; membranes; morphology; polyamides

Received 25 April 2012; accepted 21 September 2012; published online
DOI: 10.1002/app.38667

INTRODUCTION

Commercial nanofiltration (NF) and reverse osmosis (RO) thin film composites (TFCs) are primarily prepared by the interfacial polymerization of *m*-phenyldiamine (MPDA) and trimesoyl chloride (TMC).[1–4] These TFC membranes have high salt rejection properties but relatively low permeate fluxes and fouling resistance, which increases operational expenses.[5–8] In order to reduce these costs, developing TFC membranes with higher permeate fluxes while keeping their high rejections of salts is necessary.

Polyamide RO membranes that are based on MPDA/TMC exhibit high salt rejection properties but have relatively low permeate fluxes.[2,4] Interest has grown in research toward making membranes that have higher fluxes, without compromising the rejection properties. Similarly, for tight NF and RO membranes, there is a need to increase flux without loss of rejection. In addition, membranes that can be resistant to fouling and not susceptible to oxidants are also being sought. To achieve this goal, efforts to modify membrane surfaces have been made, and these include surface coating in particular by grafting.[1–3] Despite an increase in fouling resistance, salt rejection and water fluxes of coated membranes decrease.[1,5] Membrane surfaces modified through the concentration polarization-enhanced radical graft polymerization method had their permeability reduced by 20–40%, due to "caulking" defects in the polyamide layer.[6] The rejection of salts either remained the same as the unmodified membrane or slightly improved.[6]

Other efforts include those made by Hong et al. where a 4.5-bilayer poly(styrenesulfonate)/poly(allylamine hydrochloride) film was deposited on porous alumina supports,[9,10] with a sucrose and reactive dyes rejection of 99.4% and 99.9%, respectively, and NaCl salt rejection between 20% and 40%. They achieved a flux of 7.1 L m^{-2} h^{-1} at 4.8 bar, comparable to or greater than that of reported NF commercial membranes.[9,10] Wang et al. reported a triamine 3,5-diamino-*N*-(4-aminophenyl) benzamide) monomer combined with MPDA and reacted interfacially with TMC to prepare RO membranes.[11] The flux of the resultant membranes improved from 37.5 to 55.4 L m^{-2} h^{-1} as the 3,5-diamino-*N*-(4-aminophenyl) benzamide) concentration in the amine solution was increased. The rejections of the membranes were slightly decreased but the surface was more hydrophilic, smoother, and thinner.[11]

Additional Supporting Information may be found in the online version of this article.

Lind et al. prepared pure polyamide TFC and zeolite-polyamide thin film nanocomposite (TFN) RO membranes.[12] Different physical–chemical post-treatment combinations were used after the interfacial polymerization reaction to change the molecular structure of the polyamide and zeolite-polyamide thin films. Both the TFC and TFN were more permeable, hydrophilic, and rougher than the commercial seawater RO membranes. Salt rejection by the TFN membranes was lower than TFC membranes. The nearly defect-free TFN films that produced high rejections (99.4%) were achieved through wet curing with a flux of 28.1 L m^{-2} h^{-1} at 55 bar pressure.[12]

Cyclodextrins (CDs) have been used in biotechnology and bioengineering but with little application in membranes.[13] Some work has been done in making membranes for water treatment but has been used predominantly in pervaporation.[13,14] The common CDs available are α-, β-, and γ-CDs with six, seven, and eight cyclic glucose units, respectively. They are interlinked by an α-1,4 glycosidic bonds.[15] They have a high number of exterior hydroxyl groups, making them very hydrophilic and when incorporated into the polyamide thin film are expected to increase surface hydrophilicity. Making an active thin film hydrophilic have been shown to increase the permeate flux.[15,16]

Improved solvent separation with pervaporation membrane performance has been observed with the introduction of CDs.[17] For example, poly(vinyl alcohol) (PVA)/CD membranes prepared through phase inversion have been used in the separation of ethanol/water mixtures.[14,18] Polymer membranes with CD units such as poly(acrylic acid)/α-CD and PVA/β-CD were used in the separation of xylene isomers by pervaporation.[19,20] Polyrotaxanes-TiO_2-PVA (PRs-TiO_2-PVA) modified terylene membranes were prepared through dip-coating with an aqueous solution containing PR (0–3%), a derivative of α-CD, TiO_2, and PVA (1–10%) solution. The α-CDs in the PRs were meant to form inclusion complexes with a wide variety of organic pollutants.[17]

Most of the research toward improving the membrane performances has shown improved solute rejection at the expense of the permeate flux or improved permeate flux with less solute rejection.[6,21–23] A necessity, however, to develop membranes that have higher permeate fluxes, without compromising their rejection capabilities, needs to be sought. To achieve this goal, we investigated the use of amine-functionalized CDs (f-CDs) to blend the polyamide membranes. Incorporating these hydrophilic compounds onto the polyamide thin film is expected to increase the hydrophilicity of the modified TFC membranes, which could lead to higher permeate fluxes.[15,16] Amine f-CDs have cavities, which were also expected to improve the overall porosity of the polyamide thin film, resulting in membranes with improved permeate flux.[13,24] Moreover, the cavities can result in the formation of capillary channels of water through the polyamide thin film during the filtration, which could improve the permeate fluxes even higher. Through these cavities, water molecules pass through freely, but other solutes such as salts are restricted, which maintains a high rejection of the modified membranes.

In this article, polyamide TFC membrane were made from MPDA and TMC with different amounts of amino f-CDs added *in situ* to improve the permeate. This resulted in high permeate flux and high rejection properties of salts and organics.

Table I. Table Showing Different Types of Membranes with their Specific Concentrations of MPDA and Amine-f-CDs

Types of membranes	*m*-Phenyldiamine (%)	Amine f-CD (%)
A	2.0	1.5
B	2.0	1.0
C	1.5	1.5
D	1.5	1.0
E	2.0	0
F	1.5	0

EXPERIMENTAL

Materials

All chemicals used were of analytic reagent grade or higher, purchased from Sigma-Aldrich and Merck. These chemicals included sodium dodecyl sulfate, hexane, TMC and MPDA. Ultrafiltration (UF) polyethersulfone (PES) (10 kDa) membranes were supplied by Microdyn Nadir. The β-CDs were amine functionalized and characterized as previously stated.[8]

Preparation of NF/RO Membranes

PES-Radel 300 (10 kDa) UF membranes were pre-treated in sodium dodecyl sulfate (0.5%) solution overnight. The UF membranes were then washed with distilled water for 1 h, after which they were dried under the fume-hood for 2 h. They were then adhered onto a glass plate along the edges with double-sided tape together with a paper tape in order to perform the interfacial polymerization on the top dense surface of the UF membrane. A series of aqueous solutions (adjusted to pH 7, using ammonium chloride) of the f-CDs were prepared as shown in Table I.

The UF membranes were soaked for 3 h with their respective aqueous solutions. After removing excess aqueous solution from the UF membranes, the organic solution of TMC (1%) in hexane was introduced and left to stand for 60 s before curing them in an oven for 15 min, at 65°C.

Characterization of Membranes

Contact Angle Analysis. The contact angle measurements were carried out using a Dataphysics Contact Angle Instrument (SCA 20, OCA 15EC). Sessile drops of de-ionized water were measured at a rate of 12 μL/s, on dry surfaces of the membranes at room temperature. Images were captured 5 s after introducing the drop, and the contact angles were measured. Five measurements on different locations of the membrane sample were done and averaged to obtain the contact angle of the membrane.

Attenuated Total Reflectance-Fourier Transform Infrared Spectroscopy. To confirm the formation of the polyamide thin film, the attenuated total reflectance-Fourier transform infrared (ATR-FTIR) spectroscopy was used. The FTIR spectrum was collected by an ATR-FTIR Spectrometer (Perkin Elmer, Spectrum 100). The ATR-IR studies of the TFC membrane samples were carried out using a germanium crystal. The angle of incidence was fixed at 45°, and this gave a probing depth of about 0.4 μm in the IR region. The amount of contact between all the samples and crystal was the same for all the samples. Dry

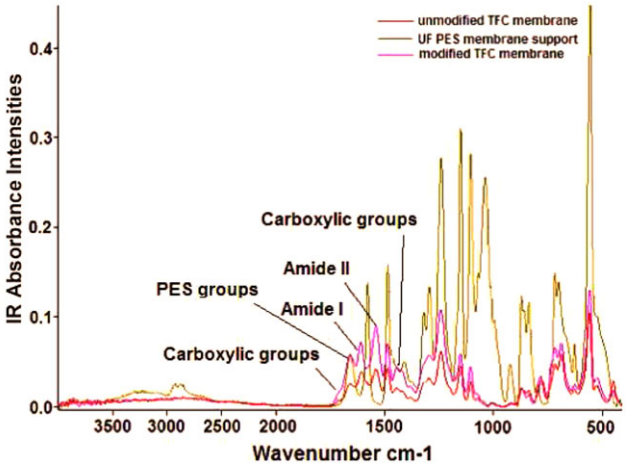

Figure 1. The ATR-IR spectra of the modified, unmodified, and UF PES support membranes. [Color figure can be viewed in the online issue, which is available at wileyonlinelibrary.com.]

specimens of membrane samples were mounted on the crystal with the active layer facing the crystal surface.

Morphological Analysis. Scanning electron microscopy (SEM) images for the membranes were taken by mounting samples on an FEI NovaNano SEM200 scanning electron microscope and irradiating them with a beam of 20 kV. Samples were frozen in liquid nitrogen and fractured for cross-section SEM analysis. All SEM samples were carbon coated. Top-view transmission electron microscopy (TEM) samples were analyzed by a JEOL JEM2100F transmission electron microscope using a dark field imaging. The polyamide thin film samples were prepared by growing them on a glass slide as described in the Experimental section. The thin films were carefully removed from the glass slide onto gelatine capsules filled with LR white resins. Samples were then mounted on carbon-coated copper grids for TEM analysis.[24] The quantitative surface roughness analysis of the composite membranes was measured by using an atomic force microscopy (AFM; Nanoscope 3D Multimode; Veeco), which utilized SNL cantilevers (Veeco) with spring constant 0.12 N/m through the contact mode on dry air. Proper magnification and accurate focusing for better viewing of the specimens were also done. Samples were dried for 12 h in a vacuum oven before AFM analysis was performed.

Permeation and Rejection Studies. The membranes were characterized by studying their permeation and rejection properties using NaCl and Na_2SO_4 (1.0 g/L) solutions. A six-cell cross-flow system was used for bench-scale water filtration experiments. Two sets of three cells each were connected in parallel to a pressure pump. After placing the membranes in the flow cells, de-ionized water was used to compress the membranes for 8 h, at 450 psi.

After 8 h, the flow rate of pure water in the membranes was determined at different pressures, and the results were used to determine the pure water permeation (J_p) by using[25]

$$J_p = \frac{V}{tAP}, \tag{1}$$

where V is the volume collected at a particular time (t), A is the active surface area of the membrane, and P is the pressure at which measurements were taken.

Feed water with specific concentrations of NaCl and Na_2SO_4 salts in 10 L was used to carry out the experiment. The filtrate was collected at a known volume and time from which the permeation was calculated using eq. (1).[25] The concentrations of the dissolved salts were determined using an electrical conductivity meter (EC-meter, Basic 30$^+$; Crison). The conductivity of the filtrate was used to compute the salt concentration from which rejection efficiencies were calculated by using[25]

$$R = 100 \times \left(1 - \frac{C_p}{C_f}\right), \tag{2}$$

where C_p is the pollutant concentration of the permeate stream and C_f is the pollutant concentration of the feed solution.

RESULTS AND DISCUSSION

ATR-IR Analysis

The modified and unmodified TFC membranes were characterized by ATR-IR spectroscopy. The germanium crystal was set to 45° angular setting to give the lowest penetration depth, while ensuring an adequate signal quality. The TFC membranes in Figure 1 shows an amide peak at 1660 cm^{-1} characteristic of amide 1 (C=O, stretch).[25] It also showed a peak at 1604 cm^{-1}, which was characteristic of the polyamide aromatic ring. A peak at 1540 cm^{-1} was characteristic of the amide II, where there is a C-N stretch.[23,26] The peaks ranging from 1000 to 1400 cm^{-1} and at 1647 cm^{-1} are characteristic of the PES UF membrane support.[26–28]

The peaks at 1450 cm^{-1} and 1734 cm^{-1} are characteristic of the carboxylic groups. This is where there is a C-O stretching, OH bending, and C=O stretching of the carboxylic groups.[27–29] Intense peaks of the carboxylic group at 1450 cm^{-1} and 1734 cm^{-1} were observed for the modified membrane, suggesting a high concentration of carboxylic groups on the membrane.[28,30] The –COCl functional groups in the TMC are involved in the crosslinking with the amine groups of the MPDA and the amine f-CDs. Since, some of the –COCl groups may not be involved in the reaction; they may be hydrolyzed to form carboxylic acids.[27,28]

SEM Analysis

The microscopic structures and morphologies of the TFC membranes studied using an FEI NovaNano SEM200 scanning electron microscope are shown in Figure 2. The membranes had a generally similar surface morphology; but roughness was different. Membranes B and D showed a high roughness. Membrane C had a dense structural surface. The roughness of the polyamide thin film of the modified TFC membranes increased due to the incorporation of the amine f-CDs; as a result, high permeate fluxes were observed.

The TFC membranes were frozen in liquid nitrogen and fractured to show the cross-section of the TFC membranes. Figure 3 shows the cross-sectional images of the unmodified membrane F and modified membrane C at 1000× magnifications.

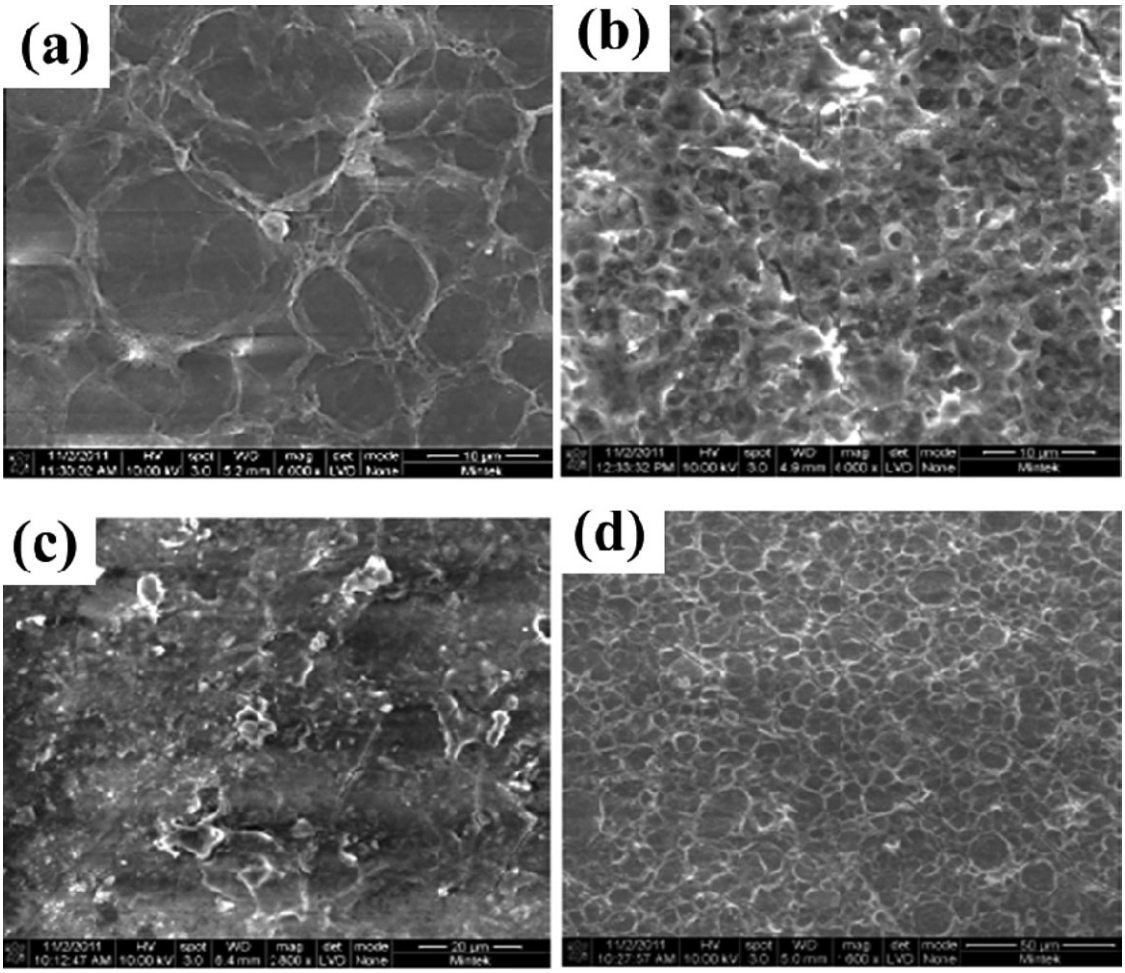

Figure 2. SEM images of TFC membranes: (a) Membrane E; (b) Membrane B; (c) Membrane C; and (d) Membrane D.

The rough edge of the TFC membranes is observed as there a clear distinction between the polyamide thin film and the PES support. There was a sharp distinction between the layers. The thickness of the unmodified thin film had an average thickness of about 6.73 μm as shown in Figure 3(a). The modified membranes have a thinner polyamide thin film of 3.27 μm, and this can explain the higher fluxes of PES as shown in Figures 7 and 8.[23]

TEM Analysis

TEM was also used to study the thin film of the modified Membrane B and unmodified membrane E (Figure 4). The polyamide thin film was grown on a glass slide, under the same conditions as the membranes on a UF PES support. The unmodified membrane was a uniform film across the surface [Figure 4(a,b)], which was dense and thicker than the modified membrane, which corresponded with the SEM image in Figure 4(a,b). Contrary to the unmodified membranes, the modified membrane polyamide thin film showed dendritic structure across the membrane [Figure 4(a,b)]. A dendritic structure was not, however, present in the unmodified membrane images. This dendritic structure is attributed to the amino f-CD incorporated into the membranes.

The dendritic structure in the modified TFC membranes was responsible for the increase in porosity and roughness of the modified membranes. It increased the total surface area of the projected surface. An increase in surface area resulted in an increase in flux.[23,31] Figure 4(d) also showed that some parts of the film are not as dense as the unmodified membrane in Figure 4(b). This explained the decrease in thickness of the modified membrane against the unmodified membrane as shown by the cross-section of the membranes (Figure 3).

AFM Analysis

The AFM analysis, an important compliment to SEM, was also used to characterize the surface morphology of the membranes. Figures 5 and 6 show the AFM images of the unmodified Membrane E and modified TFC Membrane B with projection areas of 20 μm $\times$ 20 μm. The unmodified Membrane E showed a typical nodular morphology of RO/NF membranes.[32–34] The modified Membrane B on the other hand shows a nodular dendritic structure with large macrovoids due to the presence of the CDs.

The different morphologies observed between the modified and unmodified TFC membranes may be due to the different polymerization and diffusion rates of the MPDA and amine f-CDs.[31] The interfacial polymerization to form the polyamide

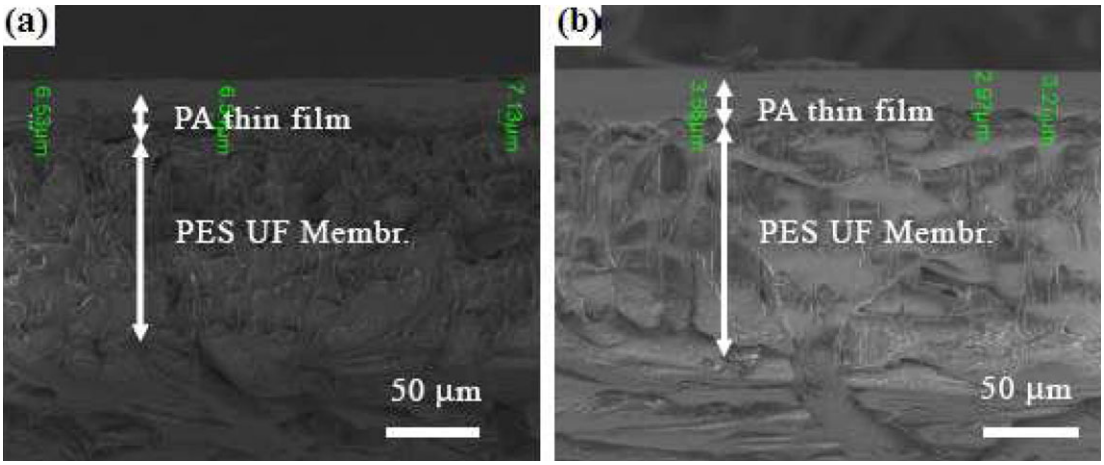

Figure 3. Cross-section SEM images: (a) Membrane F at 1000× magnification and (b) Membrane C at 1000× magnification with the polyamide thin film on top and the PES UF membrane support below. [Color figure can be viewed in the online issue, which is available at wileyonlinelibrary.com.]

thin film layer by the amines and acyl chloride in the organic phase was controlled by the amine monomer diffusion from the aqueous phase to the organic phase.[31,34] After the MPDA came into the organic phase, it reacted quickly with the TMC to form a polyamide thin film. Since the CDs are larger molecules than the MPDA, their diffusion to the organic phase was much

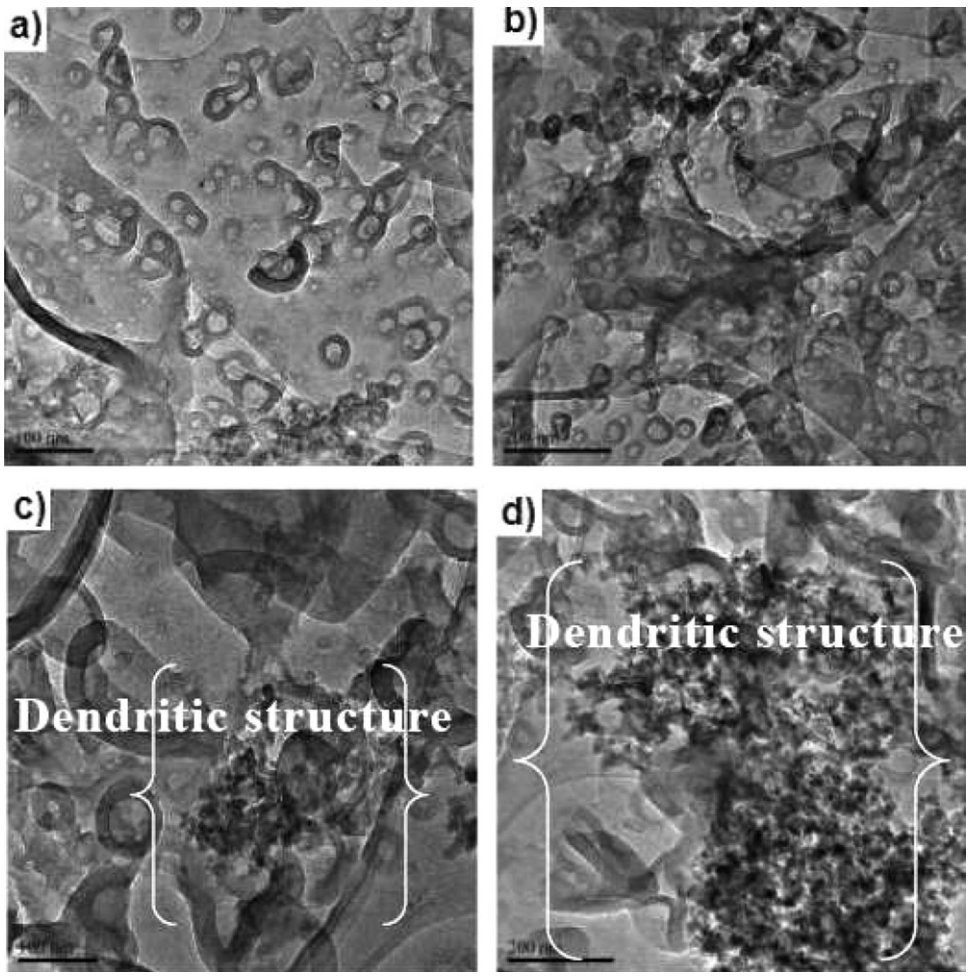

Figure 4. Top view of TEM images: (a) unmodified Membrane E (100 nm); (b) unmodified Membrane E (200 nm); (c) modified Membrane B (100 nm); and (d) modified Membrane B (200 nm).

Applied Polymer SCIENCE

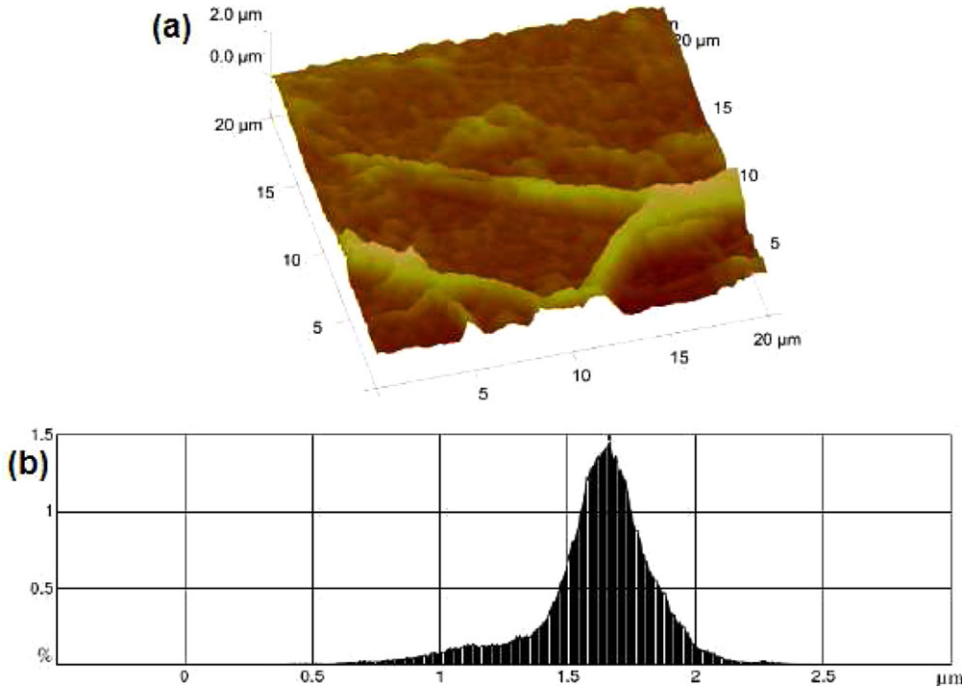

Figure 5. AFM images: (a) three-dimensional image of unmodified TFC Membrane E (20 μm × 20 μm) and (b) the peak height histogram of the image frame (20 μm × 20 μm). [Color figure can be viewed in the online issue, which is available at wileyonlinelibrary.com.]

slower, until they were prevented from further diffusion by the interfacial layer or MPDA/TMC. The amine f-CDs that reacted with the TMC to form the thin film was responsible for the porous structure of the membranes. The rest of the amine f-CDs not involved in the reaction were trapped between the active film and support pores (Figure 4). The pore sizes of the 10 kDa

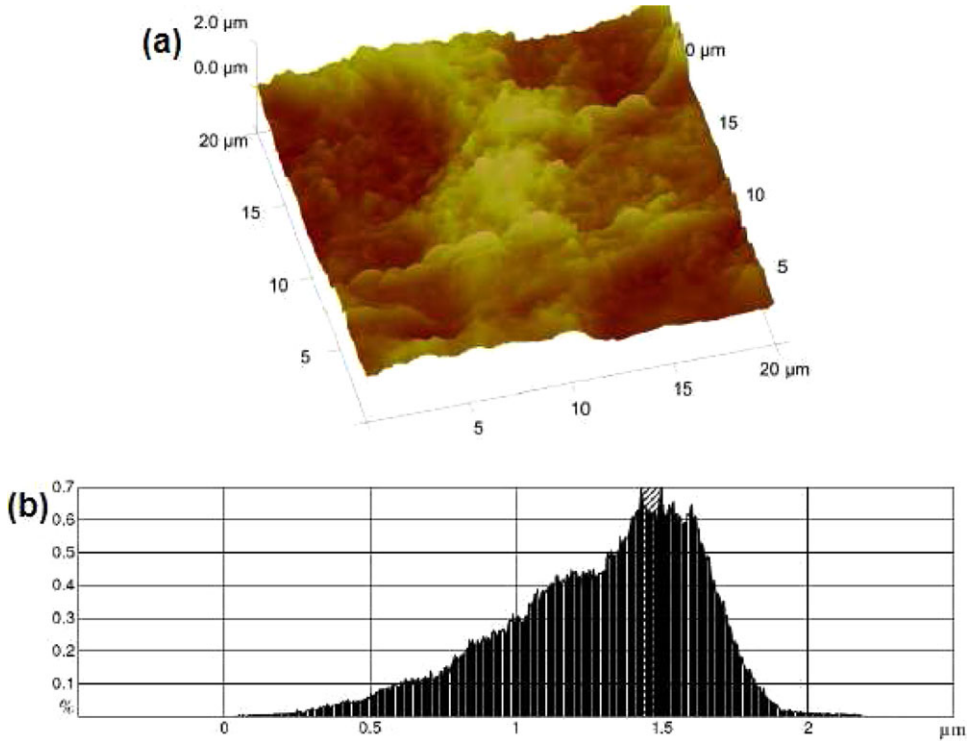

Figure 6. AFM images: (a) three-dimensional image of modified TFC Membrane B (20 μm × 20 μm) and (b) the peak height histogram of the image frame (20 μm × 20 μm). [Color figure can be viewed in the online issue, which is available at wileyonlinelibrary.com.]

Table II. The Peak to Peak Maximum Distance (S_y), Height Distribution (H_d), Average Arithmetic Roughness (R_a), Root Mean Square Roughness (R_q), and Peak Densities (P_n) of membranes

Sample identity	Image scam area	S_y (nm)	H_d (nm)	R_q (nm)	R_a (nm)	P_n
Membrane B	20 μm × 20 μm	65.3	100–2250	272	219	147
Membrane E	20 μm × 20 μm	10.8	500–2500	232	167	132

UF support membranes ranges between 100 Å and 150 Å.[32,35] The outer diameter of the β-CD was 15.3 Å, with a height of 7.9 Å.[13] Because of their smaller sizes than the pores of the UF membrane support, they caused formation of the dendritic structures on the modified membranes.

The height distribution (H_d) of the modified membranes ranged between 100 and 2250 nm at 20 μm × 20 μm area projections. The unmodified membranes had height distribution ranging between 500 and 2500 nm for the 20 μm × 20 μm area projections. The total peak density (P_n) of Membrane B was slightly more than Membrane E. The histogram of these heights of Membrane E [Figure 5(b)] showed an even distribution, whereas, for the modified membrane, it was unevenly distributed [Figure 6(b)]. This observation clearly showed an increased surface area of the modified Membrane B than unmodified Membrane E.

The surface roughness of the modified membranes was slightly higher than that of the unmodified membranes (Table II). At an area projection of 20 μm × 20 μm, the modified membranes had an average roughness (R_a) of 219 nm, higher than 167 nm of the unmodified membranes. A similar pattern was observed for the root mean roughness (R_q) and peak-to-peak maximum distance for both membranes. This shows that the modified membranes are rougher than the unmodified membranes. Other researchers have shown that the introduction of nanoparticles can result into a polymer chain nanostructure and pore size change.[32] Since, the CD nanosponges were incorporated into the polyamide film, structural changes were observed.[32]

The surface roughness of the top selective polyamide layer had been found to be directly related to membrane permeability.[23,32] The porosity of the polyamide layer arises as a result of the spaces between the chain segments within the crosslinked structure. The polymer chain nanostructure is made of a polymer network within highly dense crosslinked structures.[23] The density can be altered by solvents and nanoparticles, resulting in interconnecting and irregular pores of the polyamide membranes.[22,23]

Contact Angle and Permeate Flux

The unmodified Membranes E and F had contact angles of 59° and 60°, respectively (Figures 7 and 8). Akin and Temelli reported commercial membranes with similar contact angles between 60° and 70°.[3] These specific commercial RO membranes such as RO Membrane AK had a contact angle of 64.8° and RO Membrane AG had a contact angle of 63.5°. These contact angles are comparable to Membranes E and F prepared in this work. The modified Membranes A, B, C, and D showed lower contact angles than Membranes E and F (Figures 7 and 8). Membrane D showed a slight decrease from 60° to 56°. The rest of the modified membranes showed a considerable decrease of the contact angle. For example, Membranes A and C had a contact angle of 45°, and membrane B was 44°.

The decrease of the contact angle for the modified membranes clearly suggest an increase of the hydrophilicity of the films due to the introduction of the β-CDs.[3,36] The hydrolysis of the -COCl groups to form carboxylic acids occurred during the interfacial polymerization process in both the modified and unmodified membranes. This resulted in a decreased contact angles for both types of membranes.[27,36] The unmodified membranes had a contact angles of 60°. The modified membranes had even lower contact angles of 44° and 45°, respectively, which are attributed to the hydrophilic CDs in the polyamide thin film. Therefore, the hydrophilicity of the modified membranes was increased even further.

Membranes E and F had relatively low permeate fluxes as shown in Figures 7 and 8. Membrane E gives a permeate flux of 5.59 L m^{-2} h^{-1} at 100 psi (Figure 7) and 15.87 L m^{-2} h^{-1} at 400 psi (Figure 8). However, when comparing these permeate fluxes to the modified, a different pattern is observed. Membrane A has a

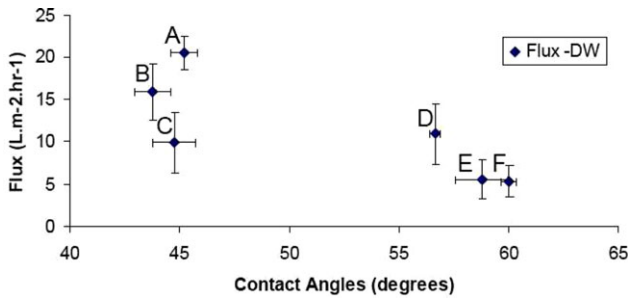

Figure 7. A comparison between the flux of de-ionized water against contact angles of TFC membranes at 100 psi. [Color figure can be viewed in the online issue, which is available at wileyonlinelibrary.com.]

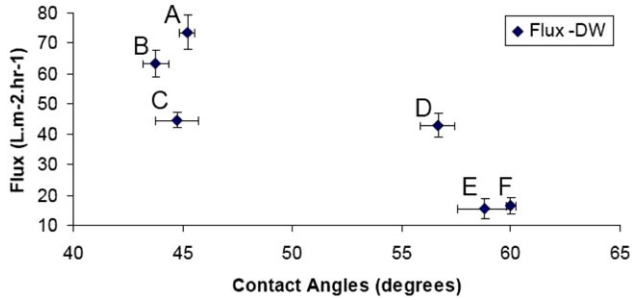

Figure 8. A comparison of the flux of de-ionized water against contact angles of TFC membranes at 400 psi. [Color figure can be viewed in the online issue, which is available at wileyonlinelibrary.com.]

Applied Polymer SCIENCE

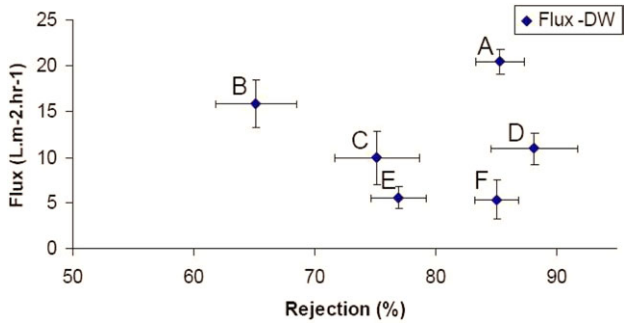

Figure 9. A graph comparing the permeate flux and the rejection of NaCl (1.00 g/L) by TFC membranes at 100 psi. [Color figure can be viewed in the online issue, which is available at wileyonlinelibrary.com.]

permeate flux of 20.48 L m^{-2} h^{-1} at 100 psi and 73 L m^{-2} h^{-1} at 400 psi. This pattern is similar for the other modified membranes against the unmodified membranes (Figures 7 and 8). This clearly shows a higher permeate flux of the modified membranes.

The modified membranes showed higher permeate fluxes than the unmodified membranes because of the incorporation of the amine f-CDs. The SEM images showed that the amine f-CDs increased the porosity of the modified membranes (Figure 3). Moreover, the AFM images show a nodular dendritic morphology of the modified membranes (Figures 6 and 7). The higher permeate flux of the modified membranes are thought to be due to the increased roughness and porosity, which in turn gives an increased surface area. A large membrane surface contacts more water in a given projected area; hence, a higher permeate flux was achieved.[31] The thickness of the modified polyamide thin layer of the membranes was thinner than the unmodified membranes, which could also give higher permeate fluxes.[13]

The hydrophilicity of the modified membranes caused by the incorporation of the hydrophilic amine f-CDs contributed to the higher fluxes.[15] Beside the hydrophilic exterior of the amine f-CDs, they also have cavities that can enhance the convective flow of water molecules. It is known that the pores of NF membranes ranges between 0.5 and 2 nm and the diameter of the β-CDs between 0.62 and 0.78 nm.[21,37] As a result, water molecules with a diameter of about 0.2 nm can pass through easily. The amine f-CDs trapped inside the pores of the UF support formed

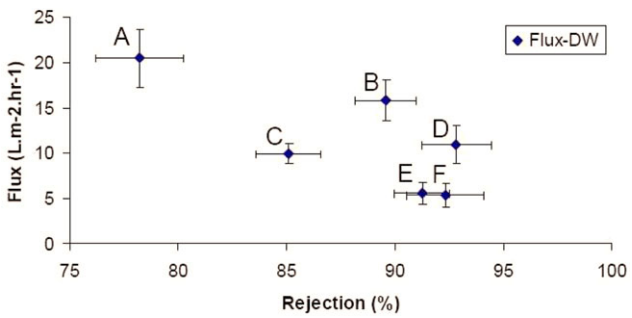

Figure 11. A comparison of the permeate flux against the rejection of Na_2SO_4 (1.00 g/L) by TFC membranes at 100 psi. [Color figure can be viewed in the online issue, which is available at wileyonlinelibrary.com.]

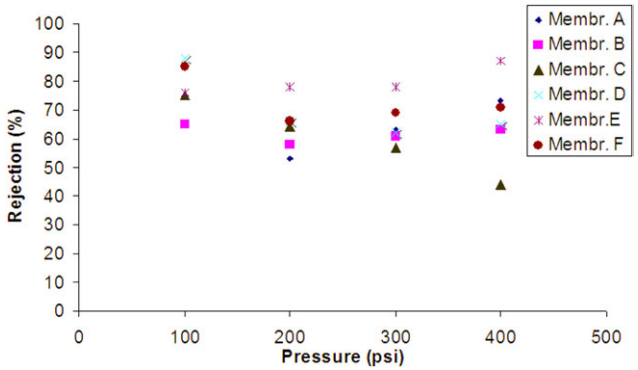

Figure 10. A graph comparing the rejection of NaCl (1.00 g/L) with increasing in pressure. [Color figure can be viewed in the online issue, which is available at wileyonlinelibrary.com.]

a dense network below the polyamide film. This dense network can be a good environment to create capillary channels for water molecules to pass through, which are large enough to allow water molecules but restrict the passage of pollutants due to particle size exclusion.[37–39]

Rejection of NaCl Salt and Permeate Flux

Sodium chloride (1.00 g/L) salt was used in this project to study the rejection efficiency of the TFC membranes. Figure 9 showed Membrane F with 85% NaCl salt rejection while Membrane E had a 77% rejection. The modified membranes such as Membrane A rejected NaCl salt at 85%. This rejection efficiency of Membrane A was comparable to Membrane F and better than Membrane E, but with a significantly better flux. Membrane B had a 65% NaCl salt rejection, which is 8% less than membrane E. Although the rejection was slightly lower for Membrane B than the unmodified membranes, the permeate flux was significantly higher. Membrane C rejected NaCl salt at 75%, which is comparable to Membrane E. Membrane D rejected at 88% of the NaCl salt. Membrane D had the highest rejection, with a higher flux than the unmodified membranes. This clearly showed that not only did the incorporation of amine f-CDs into the polyamide thin film improved permeating fluxes but also the solute rejections were not compromised.

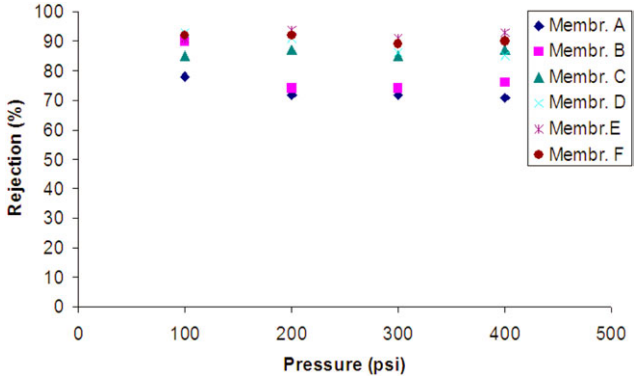

Figure 12. A comparison of the rejection of Na_2SO_4 (1.00 g/L) against increasing pressure. [Color figure can be viewed in the online issue, which is available at wileyonlinelibrary.com.]

Mazzoni et al. carried out a study where NaCl (1.17 g/L) was used to study rejection efficiencies of commercial Desal DK polyamide using pressures ranging from 2.5 to 25 bar.[24] The rejections of the Desal DK membranes reported ranged between 15% and 60%.[24] With a similar range of pressures used in this work, the flux was slightly higher than the amino f-CD modified membranes, but the rejection properties were higher (Figures 7 and 8). Figure 10 shows the rejection of NaCl salt with increasing pressure; Membrane A showed the lowest 53% NaCl rejection at 200 psi. Membrane B had the lowest rejection of 58% (NaCl salt) at 200 psi. All the membranes showed the highest rejection of up to 88%, whereas the Desal DK membranes rejected up to 60 %.[24] The modified membranes prepared in this work showed NaCl rejection efficiencies better or comparable to the unmodified membranes.

Rejection of Na_2SO_4 Salt and Permeate Flux

The rejection of the Na_2SO_4 is generally higher than the NaCl salt because of size exclusion as the diameter of Na_2SO_4 salt is higher than that of NaCl salt.[21,32,39–42] Membrane E had a 91% rejection of Na_2SO_4, whereas Membrane F had a 92% rejection (Figure 11). Membranes A, B, and C had Na_2SO_4 rejection of 78%, 89.6%, and 85%, respectively. Membrane D had the highest rejection of 94% with double higher fluxes than the unmodified membranes. As observed with the NaCl salt, the rejections of the modified membranes are comparable to the unmodified membranes, but the fluxes are significantly higher for the modified membranes (Figure 11).

The rejection distribution of Na_2SO_4 salt observed in all the membranes prepared is constant for each membrane with increasing pressure (Figure 12). The margins of the rejection efficiency were between 72 $\pm$ 2% and 94.7 $\pm$ 2% throughout the treatment process. This showed that the subjection of the membranes to different pressure did not affect the membranes' rejection efficiencies, while increasing the fluxes as shown in Figure 11.

CONCLUSION

The MPDA/TMC-based TFC membranes were successfully modified with amine f-CDs through an *in situ* interfacial polymerization reaction. ATR-IR spectrum confirmed the presence of a polyamide thin film. TEM studies demonstrate the presence of the amine f-CD polyamide polymer. The presence of the amine f-CDs in the polyamide thin film increased the porosity as shown by the SEM images. AFM showed an increase in the roughness of the modified membranes. The contact angle studies also showed that the modified membranes were more hydrophilic, which is attributed to the incorporation of the amine f-CDs. The rejection efficiencies were similar to or better than the unmodified membranes, while showing significantly improved fluxes. Flux improvement is correlated to the increased surface area, porosity, and hydrophilicity of the modified membranes due to the incorporation of the amine f-CDs. Studies to understand the mechanism of f-CDs membrane processes are underway.

ACKNOWLEDGMENTS

The authors would like to acknowledge the Department of Applied Chemistry, Faculty of Science, University of Johannesburg, and the National Research Foundation for funding, Mintek for the SEM and TEM images, Department of Desalination and Water Treatment, Ben-Gurion University of the Negev, Zuckerberg Institute for Water Research, and the Department of Chemical Engineering, Durban University of Technology, for the technical assistance provided.

REFERENCES

1. Yu, S.; Lu, Z.; Liu, X.; Liu, M.; Gao, C. *J. Membr. Sci.* **2011**, *371*, 293.
2. Petersen, R. J. *J. Membr. Sci.* **1993**, *83*, 81.
3. Akin, O.; Temelli, F. *Desalination* **2011**, *278*, 387.
4. Coronell, O.; Marinas, B. J.; Cahill, D. G. *Environ. Sci. Technol.* **2011**, *45*, 4513.
5. Kim, I. C.; Ka, Y. H.; Park, J. Y.; Lee, K. H. *J. Ind. Eng. Chem.* **2004**, *10*, 115.
6. Bernstein, R.; Belfer, S.; Freger, V. *Environ. Sci. Technol.* **2011**, *45*, 5973.
7. Freger, V.; Srebnik, S. *J. Appl. Polym. Sci.* **2003**, *88*, 1162.
8. Ghosh, A. K.; Jeong, B.-H.; Huang, X.; Hoek, E. M. V. *J. Membr. Sci.* **2008**, *311*, 34.
9. Hong, S. V.; Malaisamy, R.; Bruening, M. L. *J. Membr. Sci.* **2006**, *283*, 366.
10. Hong, S. V.; Miller, M. D.; Bruening, M. L. *Ind. Eng. Chem. Res.* **2006**, *45*, 6284.
11. Wang, H.; Li, L.; Zhang, X.; Zhang, S. *J. Membr. Sci.* **2010**, *353*, 23.
12. Lind, M. L.; Suk, D. E.; Nguyen, T. V.; Hoek, E. M. V. *Environ. Sci. Technol.* **2010**, *44*, 8230.
13. Singh, M.; Sharma, R.; Banerjee, U. C. *Biotechnol. Adv.* **2002**, *20*, 341.
14. Jiang, L. Y.; Chung, T. S. *J. Membr. Sci.* **2009**, *327*, 216.
15. Mderawan, W.; Ong, T. T.; Lee, T. C.; Young, D. J.; Ching, C. B.; Ng, S. C. *Tetrahedr. Lett.* **2005**, *46*, 7905.
16. Malaisamy, R.; Bruening, M. L. *Langmuir* **2005**, *21*, 10587.
17. Lui, L.; Xiao, L.; Yang, F. *J. Membr. Sci.* **2009**, *333*, 110.
18. Yamasaki, A.; Iwatsubo, T.; Masuoka, T.; Mizoguch K. *J. Membr. Sci.* **1994**, *89*, 111.
19. Kusumocahyo, S. P.; Kanamori, T.; Sumaru, K.; Iwatsubo, T.; Shinbo, T. *J. Membr. Sci.* **2004**, *231*, 127.
20. Chen, H. L.; Wu, L. G.; Tan, J.; Zhu, C. L. *Chem. Eng. J.* **2000**, *78*, 159.
21. Hirose, M.; Ito, H.; Kamiyam, Y. *J. Membr. Sci.* **1996**, *121*, 209.
22. Yu, S.; Lü, Z.; Chen, Z.; Liu, X.; Liu, M.; Gao, C. *J. Membr. Sci.* **2011**, *371*, 293.
23. Rao, A. P.; Desai, N. V.; Rangarajam, R. *J. Membr. Sci.* **1997**, *124*, 263.
24. Pacheco, F. A.; Pinnau, I.; Reinhard, M.; Leckie, J. O. *J. Membr. Sci.* **2010**, *358*, 51.
25. Mazzoni, G.; Bruni, L.; Bandini, S. *Ind. Eng. Chem. Res.* **2007**, *46*, 2254.

26. Coates, J.; Encyclopedia of Analytical Chemistry; Meyer R. A. Ed.; John Wiley and Sons: Newtown, **2000**; p 10815.

27. Bui, N.-N.; Lind, M. L.; Hoek, E. M. V.; McCutcheon, J. R. *J. Membr. Sci.* **2011**, 385–386, *10*.

28. Pereira, A. M. M.; Lopes, M. C.; Timmer, J. M. K.; Keurentjes, J. T. F. *J. Membr. Sci.* **2005**, *260*, 174.

29. Gupta, K. C. *J. Appl. Polym. Sci.* **1997**, *66*, 643.

30. Khulbe, K. C.; Feng, C.; Matsuura, T. *J. Appl. Polym. Sci.* **2010**, *115*, 855.

31. Li, L.; Zhang, S.; Zhang, X.; Zheng, G. *J. Membr. Sci.* **2008**, *315*, 20.

32. Singh, P. S.; Rao, A. P.; Ray, P.; Battacharya, A.; Singh, K.; Saha, N. K.; Reddy, A. V. R. *Desalination* **2011**, *282*, 78.

33. Kwak, S.-Y.; Ihm, D. W. *Colloid Surf. A* **2002**, *201*, 73.

34. Li, L.; Zhang, S.; Zhang, X.; Zheng G. *J. Membr. Sci.* **2007**, *289*, 258.

35. Singh, P. S.; Aswal, V. K. *J. Phys.* **2008**, *71*, 947.

36. Li, H.; Lin, Y.; Luo, Y.; Yu, P.; Hou, L. *J. Hazard. Mater.* **2011**, *192*, 490.

37. Vrijenhoek, E. M.; Hong, S.; Elimelech, M. *J. Membr. Sci.* **2001**, *188*, 115.

38. Adams, F. V.; Nxumalo, E. N.; Krause, R. W. M.; Hoek, E. W. M.; Mamba, B. B. *J. Membr. Sci.* **2012**, 405–406, *291*.

39. Wijmans, J. G.; Baker, R. W. *J. Membr. Sci.* **1995**, *107*, 1.

40. Cadotte, J. E.; Petersen, R. J.; Larson, R. E.; Erickson, E. E. *Desalination* **1980**, *32*, 25.

41. Shintani, T.; Matsuyama H.; Kurata, N.; Ohara, T. *J. Appl. Polym. Sci.* **2007**, *106*, 4174.

42. Song, Y.; Liu, F.; Sun, B. *J. Appl. Polym. Sci.* **2005**, *95*, 1251.